Ultraviolet Radiation Induced Dopant Loss in a TiO_2 Photo-catalyst

Nicholas P. Chadwick[a,b,], Andreas Kafizas[a, c], Raul Quesada-Cabrera[a], Carlos Sotelo-Vazquez[a], Salem M. Bawaked[d,e], Mohamed Mokhtar[d,e], Shaeel A. Al Thabaiti[d,e], Abdullah Y. Obaid[d,e], Sulaiman N. Basahel[d,e], James R. Durrant[c], Claire J. Carmalt[a*], Ivan P. Parkin[a*]

a- Materials Research Centre, Chemistry Department, University College London, WC1H 0AJ, UK

b- Bio Nano Consulting, The Gridiron Building, One Pancras Square, London, N1C 4AG

c- Chemistry Department, Imperial College London, SW7 2AZ

d- Chemistry Department, Faculty of Science, King Abdulaziz University, Saudi Arabia

e- Surface Chemistry and Catalytic Studies Group, King Abdulaziz University, Saudi Arabia

*Corresponding Authors

c.j.carmalt@ucl.ac.uk

i.p.parkin@ucl.ac.uk

Doped TiO_2's have been studied with intense interest over recent decades because of their ability to utilise visible wavelengths and enhance the efficiency of photocatalytic processes. Thus, as a class of materials, they are of significant interest for use in environmental ambient energy utilisation applications. Using a popular and well-studied form of doped TiO_2 (nitrogen doped) as an example, we show how 28 days of UVA irradiation which is identical in intensity to solar conditions is sufficient to cause the UV induced surface segregation and eventual loss of nitrogen dopant species in TiO_2. This is evidenced by X-ray photoelectron spectroscopy and transient absorption spectroscopy. The loss of interstitial nitrogen dopants correlates with the eventual permanent loss of photocatalytic activity and visible light absorption. The UV induced loss of dopants in a metal oxide is unprecedented and represents a potential problem where the environmental use of doped metal oxides in applications is concerned.

Keywords: *Photocatalysis, TiO2, Nitrogen Doping, Environment, Ultraviolet, Dopant Loss, Interstitial Nitrogen, Doped Titanium Dioxide*

Introduction

Titanium dioxide (TiO_2) is the most studied material for applications in photo-catalysis because of its high photocatalytic activity toward a range of media; including water and airborne pollutants, biological pathogens and cancer cells to highlight a few.[1,2] One drawback of TiO_2 is the wide bandgap ($\approx$ 3.2 eV), which can only absorb 3-5% of the solar spectrum in energy terms, thus limiting its suitability for usage in ambient energy utilisation applications. Many have tried to modify the structure and surface of TiO_2 to make it visible light active, with the most intensively studied being nitrogen doping first investigated by Morikawa et al.[3,4] Indeed a web of science search gives 1693 articles published in this field since 2001.

Nitrogen doping of TiO_2 results in a red shift in the bandgap towards the visible range of the electromagnetic spectrum, conferring the ability of nitrogen doped TiO_2 to carry out photo-catalysis under visible light irradiation. Whilst this has been confirmed by many within the scientific community, there are those who dispute the origins of this effect (interstitial vs substitutional doping).[5] Some argue that wholesale changes in band structure can only occur when the material is highly doped *i.e.* >10%, which cannot be said for the majority of materials examined thus far. In addition the role of nitrogen surface species has also been raised,[6] where UV driven photo-catalysis appears enhanced via stoichiometric processes and has been related to the presence of chemisorbed NH_x and interstitial nitrogen (NO), identified using EPR.[7–10] Thus, the conception that doped TiO_2 exists as a static system acting as an energy relay for electromagnetic radiation is not necessarily true.

In this report, we have performed a long-term UV-treatment study of nitrogen doped TiO_2 (*ca.* 1 month), measuring the change in surface and bulk nitrogen species with X-ray photoelectron spectroscopy (XPS) whilst also charting the change in UV photo-catalytic activity that occurs. By corroborating these results with observations from transient

absorption spectroscopy (TAS) and ultraviolet-visible absorption spectroscopy (UV/Vis), we can provide mechanistic insight on the role of nitrogen dopant species in nitrogen doped TiO_2. We demonstrate that the process of UV treatment over the course of many days causes interstitial nitrogen species in the material bulk to migrate to the surface. This resulted in a change in the TAS, where trap-states were lost, and a decrease in visible light absorption throughout the whole material. An irreversible loss of UV photo-activity was also observed. Importantly, the radiative power of UV light used in this report is similar to that experienced in normal daylight (this report uses 0.42 mW / cm^2 whilst the average UV exposure assuming a suns worth of irradiance is roughly 3 - 0.5 mW / cm^2 after atmospheric attenuation) allowing us to comment on the suitability of nitrogen doped TiO_2 for external environmental usage.[11,12]

Physical Characterisation

Pristine and nitrogen doped TiO_2 samples were synthesised using aerosol assisted chemical vapour deposition (AACVD). Specific details can be found in the experimental section. This technique conveys a degree of flexibility upon the synthesis of thin films as its main requirement is that precursor molecules are soluble in a solvent which can be easily aerosolised.[13,14] Samples shall be referred to as TiO_2 for the non-doped TiO_2 sample and N-TiO_2 for the nitrogen doped sample herein for clarity.

All films were characterised using X-ray diffraction (XRD) and found to conform to the anatase crystal structure (Figure S1 a). Little lattice expansion was observed in N-TiO_2 compared with a pristine TiO_2 sample, congruent with the incorporation of interstitial nitrogen, whose ionic radii are insufficient to cause deformation of the anatase TiO_2 lattice. An enhanced level of visible light absorption (400 - 800 nm) in N-TiO_2 compared with TiO_2 was evident from UV/Visible absorption spectroscopy (Figure S1 b). Band gap calculations, via tauc plots,[15] show that the bandgap of the N-TiO_2 is red-shifted towards the visible region of the electromagnetic

spectrum and exhibits a band gap of ~2.5 eV (Figure S1c) compared to the calculated value for pristine TiO_2 (~3.3 eV). This was also evident on a qualitative level with the N doped sample exhibiting a yellow colour compared to colourless with the undoped sample. Scanning electron microscopy (SEM) of the TiO_2 and nitrogen doped TiO_2 samples exhibit similar morphology with sharp flake-like growths observed at the surface. Both films exhibit on a qualitative level high degrees of porosity (Figure S1 d). It is important to credit the effect surface morphology can have on a material's observed rate of photo-catalysis. To compare the photocatalytic rates of materials which exhibit differing surface morphologies does not provide a full account of the effect doping has upon the generation of charge carriers. That the TiO_2 and nitrogen doped TiO_2 samples exhibit the same morphology allows dopant effects to be considered seriously in light of photo-activity data. This will be discussed in more detail later.

X-ray photoelectron spectroscopy (XPS) was undertaken to identify the oxidation state and relative concentration of titanium, oxygen and nitrogen in both N-TiO_2 and un-doped TiO_2 (Figure S1 e). Ti^{4+} species indicative of a TiO_2 environment were found in both samples, with characteristic binding energies of 458.7 eV and 464.37 eV for the $2p_{3/2}$ and $2p_{1/2}$ environments respectively.[16,17] The binding energies of the oxygen 1s environments were characteristic of Ti-O bond formation in both samples. Specifically a Ti-O-Ti linkage at 530.1 eV was seen as well as a Ti-OH surface linkage at 532.0 eV.[18,19] N-O bonds should also fall in this region, but it is well known that de-convolution of the oxygen environment is notoriously difficult and thus it will not be the centre of our argument.[20] In N-TiO_2, nitrogen was found both at the surface of the material and in the bulk through XPS depth profiling. The interstitial nitrogen environment was observed consistently throughout the material, at a binding energy of ~ 399.7 eV, which represents a nitrogen environment with no formal charge and was assigned

as NO in light of previous literature.[21-26] In the bulk, this binding energy solely represents the presence of interstitial N-O bonds. Another peak assigned as surface NO at ~401.9 eV was also observed in all samples.[24,27] No presence of substitutional nitrogen (~ 396 eV), either at the surface of the material or in the bulk, was found.[7,8,21,22,24,28,29] Another peak at ~398 eV, indicative of C-N / N-H bonds, was necessary to correctly model the XPS spectra and this is attributed to NHR_x species left over from the degradation of the nitrogen precursor.[30-32] In light of our UV-treatment studies, these XPS results will be discussed in further detail later in this report. Carbon contamination, evidenced by a peak at 282 eV representing Ti-C bonds, was present in small concentrations (on average >1%) and remained stable throughout the irradiation period of 1 month. This data is given in the supplementary information (Figure S1 f).[33]

The effect of UVA-treatment on photocatalytic activity

Photocatalytic testing was performed by charting the reduction, via a one electron process, of a resazurin dye to resorufin via a one electron reduction reaction.[34] Samples obtained from the same nitrogen doped thin film sample were irradiated using UVA light (365 nm, 0.428 mW/ cm^2) for set periods varying from 0 days to 28 days. All samples were stored in the dark for a longer period of time than investigated in this study (> 2 months), as such the sample which exhibited 0 days' worth of irradiation can be considered the baseline level, and therefore a control, of photo-activity present in all samples before irradiation. As shown in Figure 1, it was demonstrated that N-TiO₂ experienced an increase in photo-activity over the course of 7 days of UV treatment before peaking and then decreasing after 28 days treatment to a level lower than what was initially observed. The reason for this is discussed in light of XPS data later. The authors note that many studies have been conducted showing that pristine anatase TiO₂ exhibits no loss or change of activity over prolonged periods of UVA

irradiation with the work of Quesada Cabrera *et al* being of particular note.[6] No visible light activity was observed. Visible light testing was done using a Xe Arc Lamp with an intensity of 1 suns' worth of visible light irradiation. In conjunction to this a 420 nm Thor Labs cut off filter was placed between the nitrogen doped samples and the arc lamp. The test pollutant was a stearic acid thin film which has been published on widely.[6] This result was not unexpected, as the principle dopant resided in interstitial sites, which has been shown to not substantially alter the valence and conduction band energies in TiO_2 but rather should introduce mid-gap states.[7,8]
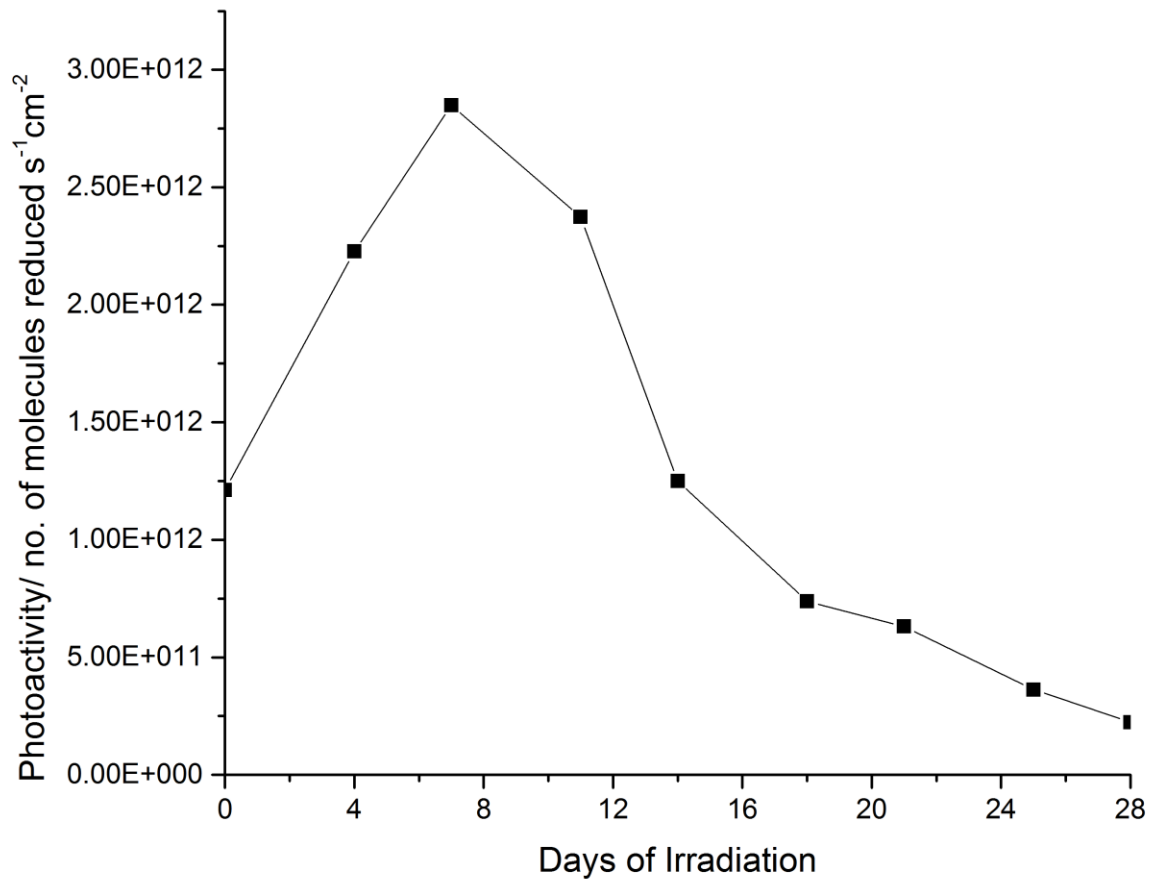

Figure 1: Photocatalytic activity in the reduction of resazurin dye in N-TiO_2 as a function of UV-treatment time (days). Activity increases from 0-7 days UV-treatment, and then decreases from 7 days treatment onwards to an activity lower than the initial level after 28 days treatment.

The Effect of UV-treatment on UV/visible Absorption and Transient Absorption Spectroscopy

Post UV-treatment, a substantial loss in absorption was observed in N-TiO$_2$ from ~400 nm into the visible region of the electromagnetic spectrum (Figure 2). This data has been normalised relative to maximum absorption in the UV to provide clear comparison between the non-irradiated and irradiated N-TiO$_2$ sample. The raw data can be found in supplementary information (Figure S1). This suggests that the species responsible for visible light absorption in N-TiO$_2$ were removed or changed as a result of prolonged UV exposure.
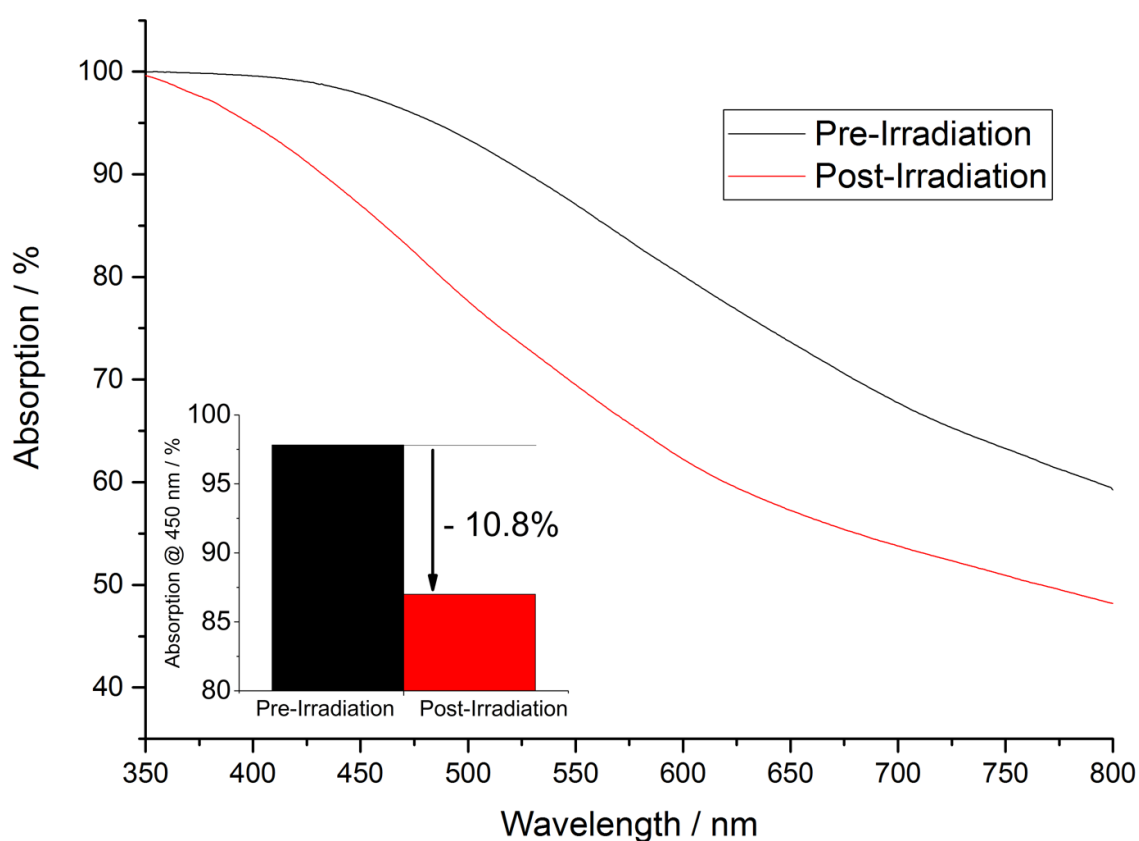

Figure 2: UV–Visible absorption spectroscopy, normalised as a percentage, of N-TiO$_2$ before and after 28 days of UV-treatment, which exhibits a significant loss in visible light absorption from ~400 nm onwards. Specifically at 450 nm a loss of 10.8% is exhibited after irradiation with UVA light of intensity similar to that found in daylight conditions.

Transient absorption spectroscopy (TAS) is a form of laser flash spectroscopy that can be used to monitor the generation, recombination, trapping and charge transfer of photo-generated charges in semiconductors. The dynamics specific to photo-generated electrons or holes can be studied by tracking transient changes in absorbance at particular wavelengths.[1]

Trapped holes absorb strongly in the near UV region (λ_{max}~500 nm) and trapped electrons absorb strongly toward the near IR (λ_{max}~800 nm).[35,36] The transient change in absorption was measured by a probe laser with a wavelength of 550, 600, 700, 800 and 900 nm following bandgap excitation at 355 nm by a laser. Measurements were done in argon (*i.e.* an inert environment). The N-TiO$_2$ sample showed similar transient decay kinetics to those observed previously in TiO$_2$.[37,38] However, the TAS of N-TiO$_2$ changed with UV treatment time (Figure 3). Before UV treatment, a negative signal (*i.e.* a bleach) was initially observed at 550 nm from 10 μs, which recovered to a positive signal by 100 μs (Figure 3, A). In anatase, this transient near-UV absorption typically corresponds to trapped hole states. However, after 28 days of UV treatment, the bleach behaviour is severely dampened (Figure 3, B), and a spectrum similar to un-doped TiO$_2$ was observed.[39] We therefore assign the bleach behaviour observed before any UVA irradiation has occurred to interstitial nitrogen states (NO) within N-TiO$_2$ trapping photo-generated electrons and by extension preserving holes, which results in the absorption feature for 550 nm seen in Figure 3A.

Comparing the time constants "t$_{50\%}$" (*i.e.* the time to reach half of the initial absorption), the speed of electron-hole recombination in N-TiO$_2$ increases from ~2 ms pre-UV treatment to ~1 ms post-UV treatment. It has previously been shown that nitrogen doping mesoporous anatase results in an increased lifetime of photo-generated charge.[40] This is due to the

formation of deeper trap-states when doping anatase with nitrogen, which protect photo-generated holes for a longer period of time before recombination occurs.
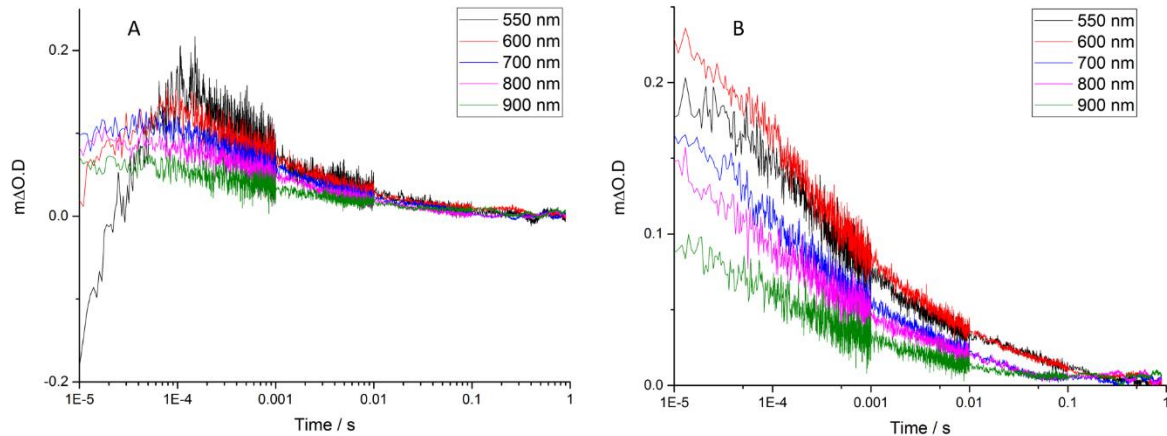

Figure 3: Transient absorption decay kinetics of N:TiO$_2$, before (A) and after (B) 28 days of UV treatment, showing the lifetime of photo-generated charge carriers for a given probe wavelength. Holes absorb strongly between 500-600 nm whilst electrons absorb at ~900 nm. Before UV-treatment, N-TiO$_2$ shows a strong bleach signal at 550 nm attributed to interstitial nitrogen dopant states trapping electrons and by extension preserving holes. Post-UV treatment, this bleach state is substantially reduced due to the irreversible loss nitrogen dopant states which can no longer accept electrons and thus recombination is increased.

Time Resolved X-ray Photoelectron Spectroscopy

X-ray Photoelectron Spectroscopy (XPS) was used to probe the change in nitrogen content, from the surface to the bulk in N-TiO$_2$ as a function of UVA irradiation time, in an attempt to link variances in interstitial nitrogen species to photo-activity and demonstrate that interstitial nitrogen doped TiO$_2$ cannot be considered a static system. Desorption surface studies of nitric oxide have regularly shown that the XPS spectrum for nitrogen exhibits an asymmetry with a shoulder present at a high binding energy (~401.9 eV) relative to the majority peak for NO at ~399.6 eV. This is assigned to physi or chemi-sorped NO species.[27,41] Concurrently, in nitrogen doped TiO$_2$ studies the peak at 399.6 eV is considered standard for interstitially doped nitrogen.[21,26,42] Therefore, the peak at 401.9 eV was assigned to surface NO species whilst the peak at 399.7 eV is representative of bulk NO. By mapping these XPS

environments separately the relationship between surface NO species at 401.4 eV and photo-activity can be elucidated and compared whilst variances in bulk concentrations of NO can also be charted to demonstrate the effect UV irradiation has upon dopant location and movement (Figure 4). Surface NO species (sN_i) and bulk NO species (bN_i) will now be discussed.
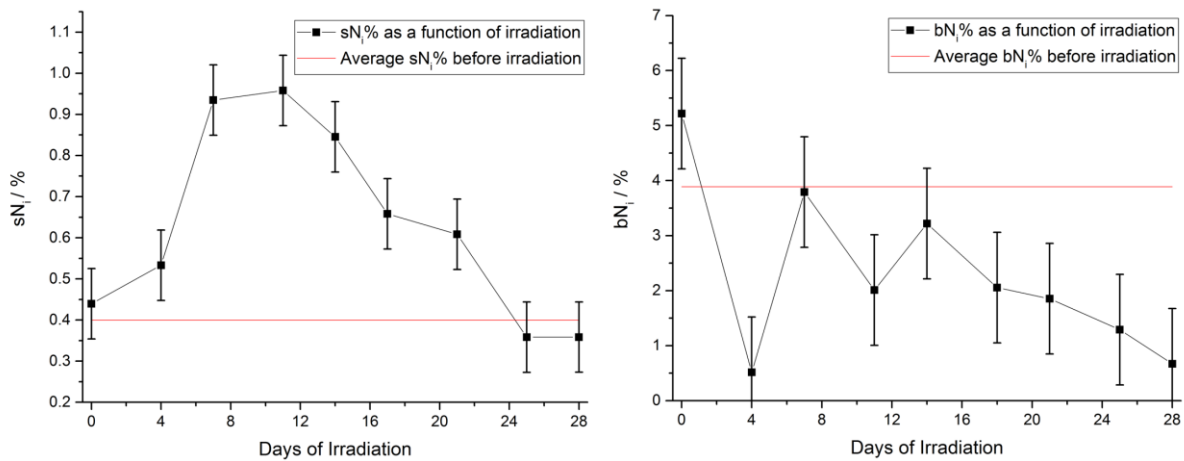

Figure 4: Graphs showing sN_i (seen at 401.9 eV in XPS) and bN_i (seen at 399.7 eV in XPS) concentration variation as a function of irradiation time (black line). The red line represents the average initial sN_i and bN_i concentrations calculated, using XPS, from many multiple points across individual samples. A standard deviation in concentration is then applied to provide insight and confidence into the quality of the data in this study.

It was observed that over 28 days of irradiation sN_i concentration increases over the first 11 days until peaking and decreasing to a level lower than pre-irradiation (Figure 4). Importantly this is identical in nature to the behaviour of surface photo-activity seen in Figure 1. Thus variances in surface NO species directly correlates with increases and changes in surface photo-activity. As no visible light activity was observed it is postulated that this process still proceeds via ultraviolet light activation since if it was purely a stoichiometric contribution results similar in nature to visible light photo-activity would be expected despite no visible light activation.

Contrastingly bN_i was observed to exhibit significant variation within the sub surface bulk across 28 days' worth of UVA irradiation (Figure 4). The concentration of bN_i prior to irradiation starts around 5% but immediately plummets to ~0.5% after four days of UVA irradiation before replenishing in the following three days to ~4%. This cycle of depletion and replenishment continues until 14 days where it was observed to decrease wholesale until 28 days. The cycle of depletion and replenishment was also observed to decrease in intensity from 0 – 14 days. Full depth profiles for all samples can be seen in Figure S2 in supplementary information. The spectra used to determine sN_i and bN_i concentrations can be found in supplementary information (Figure S3). Extra data which details the peak and eventual loss of nitrogen in previous studies at the surface of samples synthesised in the same way, but washed with deionised water, can be found in the supplementary information (Figure S4). The phenomenon is therefore repeatable.

It is well known that TiO_2 can photo-catalyse the oxidation of surface NOx species to nitric acid for applications in air purification and the mechanisms and reaction pathways have also been identified.[43–46] Therefore we hypothesise that interstitial dopant (N-O*) loss is via a mechanism similar to those already established. The formal characterisation of the acid product, whilst not the subject of this paper, requires further work. We also argue that once these surface interstitial nitrogen species are oxidised, and the acid product removed through weathering (*i.e.* reactions with water or atmospheric moisture), more interstitial nitrogen species migrate from the bulk to the surface and are once more oxidised. We make this assertion based on the surface fluctuation of bN_i states seen in Figure 4. The exact mechanism by which this occurs is unknown and requires further work to elucidate its true nature. This could be facilitated by the high mobility of the interstitial nitrogen species in $N-TiO_2$, given their size and zero associated charge on the nitrogen centre (*i.e.* a weaker bond strength than

substitutional nitrogen states, N^{3-}).[22,24] This cycle of surface migration of interstitial nitrogen from the bulk, and its oxidation and removal from the surface continues until the overall doping level of interstitial nitrogen is substantially reduced, which results in a loss of visible light absorption (as the mid-gap absorption state is lost); as evidenced by UV-visible spectroscopy and TAS studies. Photo-catalysis may be enhanced if holes are better preserved through NO_x oxidation reactions at the surface, then the electrons will be more available for surface reactions with the resazurin dye used in photo-activity measurements. While it is not the aim of this report to remediate this attrition of dopants but to characterise it for the first time, further work may take the form of using capping layers to arrest the observed loss. Another strategy may be to focus on substitutional doping for environmental applications, as the covalent bonding found in such a system should in theory prohibit the observations disclosed in this report.

Conclusion

In conclusion we have made a nitrogen doped TiO_2 sample solely doped with interstitial nitrogen by AACVD. We have assessed the effect of UV-treatment, using a 365 nm light source of a similar power to the UVA content of sunlight in the UK (0.42 mW / cm^2). We observed a temporary increase in photocatalytic activity that is inevitably and permanently lost. We attribute this variance to enhanced scavenging of photo-generated holes by surface nitrogen species and thus better reactivity between our dye and the photo-generated electrons that remain. After the month of UV-treatment the level of photo-activity resides substantially below its initial level, thus we report an irreversible loss of function. Congruent with this loss of functionality exists a loss of visible light absorption (UV-vis) and loss of nitrogen trap states and a change in the recombination behaviour (TAS). This is corroborated by time resolved XPS which showed that surface NO species correlate with changes in photo-activity and bulk NO

species exhibit a cycle of depletion and replenishment before exhibiting a wholesale decrease in nitrogen content over the period of a months' worth of irradiation. We hypothesise that this loss of interstitial nitrogen through the surface is closely related to the well documented phenomenon of NO_x oxidation by pristine TiO_2.

Our findings demonstrate the need for long term testing within the community to ascertain the true suitability of a material for use in environmental applications. Whether this effect can be replicated in other doped metal oxide systems remains to be seen and this therefore requires further investigation.

Methods

Thin film Preparation using AACVD

Nitrogen (99.99%) (BOC) was used as supplied. Depositions were obtained on SiO_2 coated float-glass. Prior to use the glass substrates were cleaned using water, isopropanol and acetone and dried in air. Glass substrates of ca. 4.5 cm x 15 cm x 4 mm were used. The precursors, titanium (IV) isopropoxide (99%) and n-butylamine (99%) were obtained from Sigma-Aldrich Chemical Co. and used as supplied. Aerosols were generated in absolute ethanol (99%) and carried into the reactor in a stream of nitrogen gas through a brass baffle to obtain a laminar flow. A graphite block, containing a Whatmann cartridge heater, was used to heat the glass substrate. The temperature of the substrate was monitored using a Pt–Rh thermocouple. Depositions were carried out by heating the horizontal bed reactor to the required temperature of 500 °C before diverting the nitrogen line through the aerosol and hence to the reactor. The total time for the deposition process took ~40 minutes. At the end of the deposition, under the nitrogen flow, the glass substrates were left to cool to room temperature with the graphite block before it was removed. The solution based ratio of nitrogen: titanium in the nitrogen doped sample (N-TiO_2) was 2:1 which equated to 0.5 g of titanium (IV) isopropoxide in 20 ml of ethanol and 3.6 ml of n-butylamine. An undoped TiO_2 sample was also synthesised in the same way to allow comparison.

Sample Characterisation

X-ray diffraction (XRD) was carried out using a Lynx-Eye Bruker X-ray diffractometer with a mono-chromated Cu Kα (1.5406 Å) source. X-ray photoelectron spectroscopy (XPS) was carried out using a Thermo Scientific K-Alpha

instrument with monochromatic Al-Kα source to identify the oxidation state and chemical constituents. High resolution scans were done for the Ti (3d), N (1s), O (1s) and C (1s) at a pass energy of 40 eV. The peaks were modelled using Casa XPS software with binding energies adjusted to adventitious carbon (284.5 eV). SEM images were taken on a JEOL JSM-6301F Field Emission instrument with acceleration voltage of 5 kV. Images were captured using SEMAfore software. Samples were cut into coupons representing the different timed samples and coated with a fine layer of gold to avoid charging. The optical transmission was measured over 320–800 nm range using a Lamda 950 UV/Vis spectrometer. Transient absorption spectroscopy was carried out using a custom built setup under an inert atmosphere (N_2) and utilised a pump wavelength of 355 nm and probe wavelength range from 500-900 nm.

Functional Property Testing

Visible light induced photo-catalytic activity was assessed using an established method based on the hydroxyl radical induced mineralisation of stearic acid and UV photo-activity was assessed via the reduction of a resazurin dye. Samples were dip coated into a stock solution of stearic acid in chloroform at a rate of 60 cm/minute, one side was wiped clean and the sample mounted on an aperture to facilitate irradiation and IR spectroscopy. The visible light source was a Xe Arc Lamp with an intensity of 1 suns worth of visible light intensity. A 420 nm Thor Labs cut off filter was also used to filter out UVA wavelengths. The resazurin based ink was evenly applied using a spray gun and the photo-induced degradation of the resazurin ink monitored by UV-Vis spectroscopy. The number of molecules destroyed per s per cm^2 by the photon flux (4.53 x 10^{14} photons per cm^2 per s) was then calculated.

Acknowledgements

Author contributions

N.P.C designed and conducted the majority of the experiments. A.K conducted TAS experiments and helped discuss and analyse data. R.Q.C and C.S.V. helped with experimental design and discussion of data. S.M.B and M.M. were involved in a number of scientific discussions and analysis of results. S.N.B generated ideas and spearheaded the initial collaboration between the institutions. A.Y.O and S.A.A were involved with a number of scientific discussions and analysis of results and have provided valuable insights, which have in turn, directed the research. J.R.D. provided the TAS equipment and C.J.C and I.P.P provided lab space, machinery and useful discussion in designing and analysing experiments.

Supporting Information

- Figure S1: XRD, UV/Vis spectroscopy, Tauc Plots, SEM and XPS for characterisation of nitrogen doped TiO_2.

- Figure S2: XPS Depth profiling data for UVA irradiation study.

- Figure S3: Fitted N1s XPS spectrums for all samples.

- Figure S4: Extra irradiation data

Competing interests
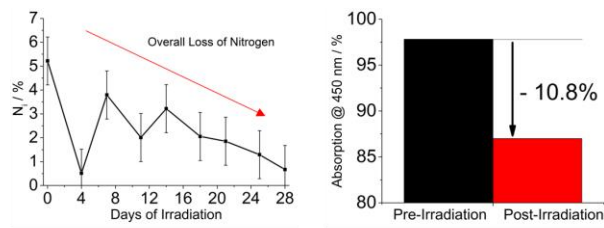
The authors declare no competing financial interests

References

(1) Fujishima, A.; Zhang, X.; Tryk, D. *Surf. Sci. Rep.* **2008**, *63* (12), 515.

(2) Mills, A.; Le Hunte, S. *J. Photochem. Photobiol. A Chem.* **1997**, *108* (1), 1–35.

(3) Zhang, H.; Chen, G.; Bahnemann, D. W. *J. Mater. Chem.* **2009**, *19* (29), 5089.

(4) Morikawa, T.; Asahi, R.; Ohwaki, T.; Aoki, K.; Taga, Y. *Jpn. J. Appl. Phys.* **2001**, *40* (Part 2, No. 6A), L561–L563.

(5) Quesada-Cabrera, R.; Sotelo-Vázquez, C.; Quesada-González, M.; Melián, E. P.; Chadwick, N.; Parkin, I. P. *J. Photochem. Photobiol. A Chem.* **2017**, *333*, 49–55.

(6) Quesada-Cabrera, R.; Sotelo-Vazquez, C.; Darr, J. A.; Parkin, I. P. *Appl. Catal. B Environ.* **2014**, *160–161*, 582–588.

(7)   Di Valentin, C.; Pacchioni, G.; Selloni, A.; Livraghi, S.; Giamello, E. *J. Phys. Chem. B* **2005**, *109* (23), 11414–11419.

(8)   Di Valentin, C.; Finazzi, E.; Pacchioni, G.; Selloni, A.; Livraghi, S.; Paganini, M. C.; Giamello, E. *Chem. Phys.* **2007**, *339* (1–3), 44–56.

(9)   Napoli, F.; Chiesa, M.; Livraghi, S.; Giamello, E.; Agnoli, S.; Granozzi, G.; Pacchioni, G.; Di Valentin, C. *Chem. Phys. Lett.* **2009**, *477* (1), 135–138.

(10)   Emeline, A. V.; Kuznetsov, V. N.; Rybchuk, V. K.; Serpone, N. *Int. J. Photoenergy* **2008**, *2008*, 1–19.

(11)   Willson, R. C. *Geophys. Res. Lett.* **2003**, *30* (5), 1199.

(12)   Kopp, G.; Lean, J. L. *Geophys. Res. Lett.* **2011**, *38* (1).

(13)   Hou, X.; Choy, K. L. *Chem. Vap. Depos.* **2006**, *12* (10), 583–596.

(14)   Marchand, P.; Hassan, I.; Parkin, I. P.; Carmalt, C. J. *Dalton Trans.* **2013**, *42* (26), 9406–9422.

(15)   Tauc, J. *Mater. Res. Bull.* **1968**, *3* (1), 37–46.

(16)   Slink, W. *J. Catal.* **1981**, *68* (2), 423–432.

(17)   Fierro, J. L. G.; Arrua, L. A.; Lopez Nieto, J. M.; Kremenic, G. *Appl. Catal.* **1988**, *37*, 323–338.

(18)   Atashbar, M. Z.; Sun, H. T.; Gong, B.; Wlodarski, W.; Lamb, R. *Thin Solid Films* **1998**, *326* (1–2), 238–244.

(19)   Wang, Y.; Feng, C.; Zhang, M.; Yang, J.; Zhang, Z. *Appl. Catal. B Environ.* **2010**, *100* (1–2), 84–90.

(20)   Shuxian, Z. *J. Catal.* **1986**, *100* (1), 167–175.

(21)   Kafizas, A.; Crick, C.; Parkin, I. P. *J. Photochem. Photobiol. A Chem.* **2010**, *216* (2–3), 156–166.

(22)   Hu, X.; Tu, R.; Wei, J.; Pan, C.; Guo, J.; Xiao, W. *Comput. Mater. Sci.* **2014**, *82*, 107–113.

(23)   Finazzi, E.; DiValentin, C.; Selloni, A.; Pacchioni, G. *J. Phys. Chem. C* **2007**, *111* (26), 9275–9282.

(24)   Palgrave, R. G.; Payne, D. J.; Egdell, R. G. *J. Mater. Chem.* **2009**, *19* (44), 8418.

(25)   Lee, S.; Cho, I.-S.; Lee, D. K.; Kim, D. W.; Noh, T. H.; Kwak, C. H.; Park, S.; Hong, K. S.; Lee, J.-K.; Jung, H. S. *J. Photochem. Photobiol. A Chem.* **2010**, *213* (2–3), 129–135.

(26)   Zeng, L.; Song, W.; Li, M.; Jie, X.; Zeng, D.; Xie, C. *Appl. Catal. A Gen.* **2014**, *488*, 239–247.

(27)   Baird, R. J.; Ku, R. C.; Wynblatt, P. *Surf. Sci.* **1980**, *97* (2–3), 346–362.

(28)   Tarasov, A.; Minnekhanov, A.; Trusov, G.; Konstantinova, E.; Zyubin, A.; Zyubina, T.; Sadovnikov, A.; Dobrovolsky, Y.; Goodilin, E. *J. Phys. Chem. C* **2015**, *119* (32), 18663–18670.

(29)   Chen, H.; Nambu, A.; Graciani, J.; Hanson, J. C.; Fujita, E.; Rodriguez, J. A. *J. Phys. Chem. C* **2007**, *111* (3), 1366–1372.

(30)   Aarons, L. J.; Barber, M.; Connor, J. A.; Guest, M. F.; Hillier, I. H.; Ikemoto, I.; Thomas, J. M.; Kuroda, H. *J. Chem. Soc. Faraday Trans. 2* **1973**, *69* (0), 270.

(31)   Peden, C. H. F.; Rogers, J. W.; Shinn, N. D.; Kidd, K. B.; Tsang, K. L. *Phys. Rev. B* **1993**, *47* (23), 15622–15629.

(32)   Feng, D.; Zhou, Z.; Bo, M. *Polym. Degrad. Stab.* **1995**, *50* (1), 65–70.

(33) Galuska, A. A.; Uht, J. C.; Marquez, N. *J. Vac. Sci. Technol. A Vacuum, Surfaces, Film.* **1988**, *6* (1), 110.

(34) Mills, A.; Wang, J.; Lee, S.-K.; Simonsen, M. *Chem. Commun. (Camb).* **2005**, No. 21, 2721–2723.

(35) Kafizas, A.; Wang, X.; Pendlebury, S. R.; Barnes, P.; Ling, M.; Sotelo-Vazquez, C.; Quesada-Cabrera, R.; Li, C.; Parkin, I. P.; Durrant, J. R. *J. Phys. Chem. A* **2016**, *120* (5), 715–723.

(36) Yoshihara, T.; Katoh, R.; Furube, A.; Tamaki, Y.; Murai, M.; Hara, K.; Murata, S.; Arakawa, H.; Tachiya, M. *J. Phys. Chem. B* **2004**, *108* (12), 3817–3823.

(37) Cowan, A. J.; Leng, W.; Barnes, P. R. F.; Klug, D. R.; Durrant, J. R. *Phys. Chem. Chem. Phys.* **2013**, *15* (22), 8772–8778.

(38) Tang, J.; Durrant, J. R.; Klug, D. R. *J. Am. Chem. Soc.* **2008**, *130* (42), 13885–13891.

(39) Wang, X.; Kafizas, A.; Li, X.; Moniz, S. J. A.; Reardon, P. J. T.; Tang, J.; Parkin, I. P.; Durrant, J. R. *J. Phys. Chem. C* **2015**, *119* (19), 150423173617003.

(40) Tang, J.; Cowan, A. J.; Durrant, J. R.; Klug, D. R. *J. Phys. Chem. C* **2011**, *115* (7), 3143–3150.

(41) Palgrave, R. G.; Payne, D. J.; Egdell, R. G. *J. Mater. Chem.* **2009**, *19* (44), 8418.

(42) Powell, M. J.; Palgrave, R. G.; Dunnill, C. W.; Parkin, I. P. *Thin Solid Films* **2014**, *562*, 223–228.

(43) Devahasdin, S.; Fan, C.; Li, K.; Chen, D. H. *J. Photochem. Photobiol. A Chem.* **2003**, *156* (1–3), 161–170.

(44) Squadrito, G. L.; Pryor, W. A. *Free Radic. Biol. Med.* **1998**, *25* (4–5), 392–403.

(45) Freitag, J.; Domínguez, A.; Niehaus, T. A.; Hülsewig, A.; Dillert, R.; Frauenheim, T.; Bahnemann, D. W. **2015**, *119* (9), 4488–4501.

(46) Zhang, M.; Li, C.; Qu, L.; Fu, M.; Zeng, G.; Fan, C.; Ma, J.; Zhan, F. *Appl. Surf. Sci.* **2014**, *300*, 58–65.

Graphical Abstract